

A Parametric Workflow for Brazing-Ready, Self-Supporting Metal AM Components with Recoverable Features

Andrei-Alexandru Popa, Fatma Nur Depboylu

Institute of Mechanical and Electrical Engineering (IME), SDU Mechatronics (Centre of Industrial Mechanics), University of Southern Denmark, DK-6400, Sønderborg, Denmark

Abstract

This study introduces a semi-automated workflow for generating self-supporting metal AM structures for torch and vacuum brazing. Maintaining contact and alignment during brazing is critical—particularly for large, complex assemblies where conventional fixturing is costly, wasteful, and shape-specific. Leveraging the design freedom of AM, sacrificial and recoverable features are embedded directly into parts and generated via a Grasshopper 3D visual programming interface. Users can tune up to four geometric parameters to rapidly create application-specific support geometries. The workflow enables interference fits with adjustable offsets for various filler materials. Sacrificial features are designed to be re-powderized into feedstock, reducing waste. Joints fabricated using this method have been mechanically characterized to assess strength and reliability under relevant loading conditions. Preliminary results demonstrate strong potential for scaling this approach into a fully generative design method, enabling self-supporting joints and large monolithic components—as seen in fusion systems—to be produced without external fixtures.

Introduction

Among joining methods, with roots traceable to Anginet Egypt, brazing stands out as the oldest and most versatile technique (Roberts, 2013). In brazing, maintaining precise contact and alignment between mating components is critical to achieving high-strength, void-free joints. This requirement becomes especially pronounced in metal assemblies exposed to demanding thermal or mechanical conditions, such as those used in aerospace, fusion energy systems, and other advanced engineering applications (Martin, 1968; F. Delzendehrooy, 2022). Traditional brazing methods rely on dedicated external fixtures to secure parts during the heating cycle (Dryden, 1982). However, such fixtures are typically costly, geometry-specific, and impractical for large or nonstandard parts—particularly when scaling up production or dealing with one-off or highly complex assemblies.

Additive manufacturing (AM), through its virtually limitless design space, presents an opportunity to rethink this paradigm. The geometric freedom inherent to metal AM enables the integration of support features directly into components, potentially eliminating the need for separate fixtures. Yet, in practice, brazing of AM parts still commonly involves legacy approaches, which underutilize the design potential of digital fabrication workflows. This mismatch introduces inefficiencies in material use, labor, and process scalability (Dryden, 1982)

To address these challenges, this study introduces a semi-automated, parametric workflow for embedding self-supporting features directly into metal AM components intended for both vacuum and torch brazing. These features are designed to ensure proper contact and alignment during brazing without the need for external fixturing. The workflow enables the generation of custom, application-specific presets, tailored for either vacuum or torch brazing conditions, with tunable geometric parameters to suit filler materials, joint types, and thermal constraints. Generative features in structural modelling, while not yet a paradigm, can be traced back to over a decade ago (Chi, Wang, & Jiao, 2015). Most popular in the architectural community (Liao, Lu, Fei, Gu, & Huang, 2024), generative designs have also entered the engineering application space (NASA, 2025). There is, however, little published work on generative design intended for multi-process or hybrid manufacturing. Optimized, machine learning designs for brazing have targeted chemical composition rather than structural aspects (Fang, et al., 2024).

Self-supporting features include both sacrificial and recoverable elements. Post-brazing, these can be removed and re-powderized into usable feedstock similarly to bulk components (Lanzutti & Marin, 2024), minimizing material waste and contributing to circular manufacturing practices. The mating geometry also

supports interference fits, with adjustable offsets to account for expansion and shrinkage effects during brazing. (Ebnesajjad, 2014). The process is implemented using visual programming in Grasshopper 3D (Grasshopper3D, 2025), allowing users to intuitively control up to four key geometric parameters in a fast and flexible environment. While the current workflow requires operator input, it significantly reduces design time and serves as a foundation for future full automation.

Advances in CAD and visual programming now make it feasible to embed manufacturing-aware intelligence directly into part design. Looking forward, this semi-automated approach could be extended using machine learning techniques to create a fully generative workflow—automatically selecting feature parameters based on part geometry, historical performance data, and expected joint conditions.

To assess the feasibility of this approach, we inspected and mechanically characterized brazed joints fabricated using the proposed method, evaluating strength and performance under relevant loading conditions. The results demonstrate that the embedded features maintain joint integrity and alignment, and that the method is scalable to larger monolithic assemblies, such as those required in fusion systems. This work establishes a pathway toward smarter, more sustainable, and fixtureless brazing solutions in metal AM.

Materials and Methods

To evaluate the proposed semi-automated workflow, we selected a model use case involving the joining of metal tensile specimen halves, each of 52.5 mm in height, Ø10mm in diameter and with a 12.55 mm gauge length. These parts are inherently asymmetrical, flattened on one side of the grip section and rounded, to purposely create alignment and stabilization challenges during brazing. While not large or highly complex, these geometries exhibit critical characteristics—such as lack of flat reference surfaces, inherent unbalance and limited contact area—that are representative of the difficulties encountered in larger or more intricate structures. As such, this use case serves as a scalable proxy for more demanding joining scenarios involving butt-joint interfaces and monolithic assemblies. The approach is not limited to butt-joints, as shown in Figures x and y, nor the shape of the locking mechanism (Figures z, t). The butt-joint use case is selected as it better highlights the versatility of the proposed solution with respect to torch and vacuum brazing. Interference joints can benefit equally from the workflow in the case of the former, while the latter's dependence on inserted filler films has yet to be handled.

2.1 Additive Manufacturing Setup

All components, including the tensile specimens and self-supporting features, were fabricated using 316L stainless steel powder supplied by Sandvik (Sandvik, 2025). Fabrication was performed on an Xact Metal XM200G (Xact Metal, 2025) laser powder bed fusion (L-PBF) system. The selected material is widely used for structural applications and brazing studies due to its corrosion resistance, mechanical strength, and printability. The choice is further justified given its relative simplicity of brazing, the focus therefore being maintained on the performance on the generated support structure and its integration into the joining experience.

2.2 Digital Workflow Architecture

The digital design and generation of the support and mating features were performed using Grasshopper 3D, a visual programming language embedded in the Rhino CAD environment. The workflow is semi-automated, and requires an operator to choose the target geometry to be imported (in this case, one half of a tensile specimen) and define a few critical parameters. The process produces two STL files—a male and a female counterpart—each with all necessary supporting and alignment features integrated, ready for slicing and 3D printing.

Four key features were identified as essential for achieving fixtureless brazing:

Anchor Base Plate:

A custom platform is generated at the base of the part to support the gauge section of the tensile specimen. This is crucial because the gauge section hangs unsupported in the build and would otherwise be prone to warping or misalignment.

Interface Pins:

Pins are generated between the anchor plate and the specimen's outer surfaces. These pins are placed in both the XZ and YZ planes to maintain multi-axis stability during printing and brazing. They are designed to be mechanically weak for easy removal post-brazing and are recoverable for re-powderization into feedstock, contributing to material circularity.

Anti-Roll Plates:

Lateral fins are added to the structure to prevent rolling or lateral displacement of the specimen. These provide additional stabilization without interfering with the print path or post-processing. The trapezoidal shape is predefined in software to minimize material usage and simplify subsequent support removal, by not exceeding a 45 degree overhang threshold.

Locking Mechanism:

A male-female alignment feature is introduced at the butt-joint interface. This mechanism provides self-centering during assembly and maintains contact during brazing. The male-female geometry includes a tunable offset to accommodate different filler materials. For torch brazing, the offset can either be null or set to a desired value, while vacuum brazing typically relies on a filler film which implies the need for an accommodating gap.

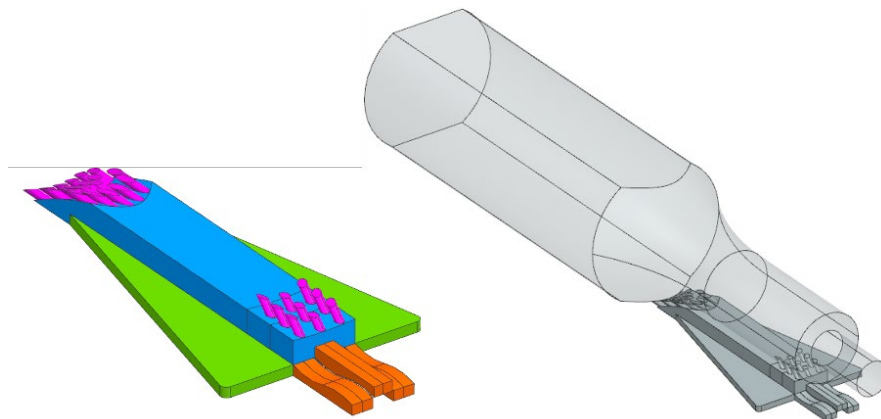


Figure 1 - Support steps, including anchor (blue), interface (magenta), anti-roll plate (green) and locking mechanism (orange)

2.5 Workflow Sequence

The user begins by importing the target specimen geometry into the Grasshopper environment. The part is oriented to define the build direction, after which interface pins are projected to the outer boundaries. The anchor plate is generated atop these pins, and the pins are trimmed by a boolean to integrate into the plate geometry. Next, the anti-roll features are added as lateral extensions.

Once support for a single half is complete, the locking mechanism is added to the interface surface, creating either a male or female version depending on the part's designation. The mechanism's offset and tolerances are adjustable via exposed parameters, allowing customization for different brazing conditions. Figure 3 reveals the UI for all operator selections. The final output consists of paired STL files (male and female), complete with sacrificial and alignment features, ready for slicing and printing. Figure 2 highlights the steps of the proposed workflow.

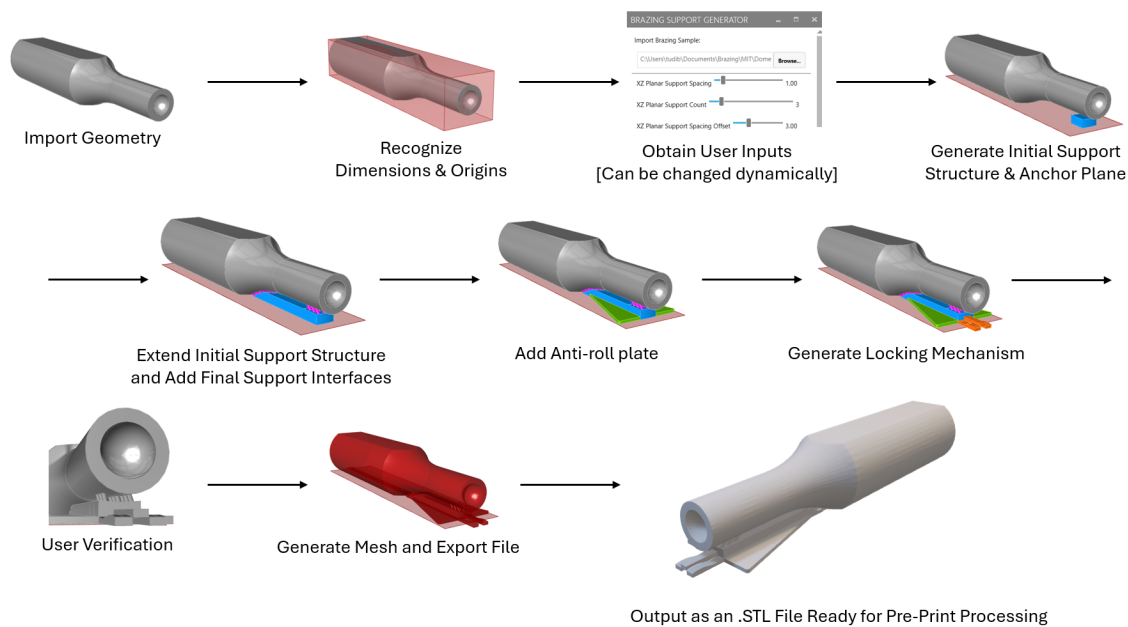


Figure 2 - Workflow sequence

This process is directly extensible to other geometries beyond tensile specimens, including half-dogbones, cylindrical segments, or even customized, large-scale monolithic components. While currently semi-automated, this parameterized workflow lays the groundwork for future integration with machine learning algorithms, which could predict optimal feature configurations based on part geometry and historical performance data.

Results and Discussions

To evaluate the functionality and effect of different support configurations, two parameter sets (V1 and V2) were developed by tuning the four geometric parameters defined in the workflow. Each parameter set was applied to a **butt-jointed tensile specimen** with two variants—one featuring **no offset** and the other a **0.1 mm offset** at the locking interface (see **Figure 3**).

The workflow steps highlighted in Figure 2, while not directly applicable to any other geometry, empower the user to handle virtually any class of tensile specimens. The selection of parameters between sets V1 and V2 is not arbitrary. While the stability of each of the parts is guaranteed by the anti-roll plate, the quality of the braze is expected to be more directly influenced by the locking mechanism and the interface pins. As such, the tolerances between the male and female interference elements are modified through a scaling factor (0.48 for V1, 0.55 for V2). The relatively small change is chosen as testimony to the sensitivity of the process to adequate parametrization. The length and number of pins would affect the artefacts on the surface, and is therefore varied.

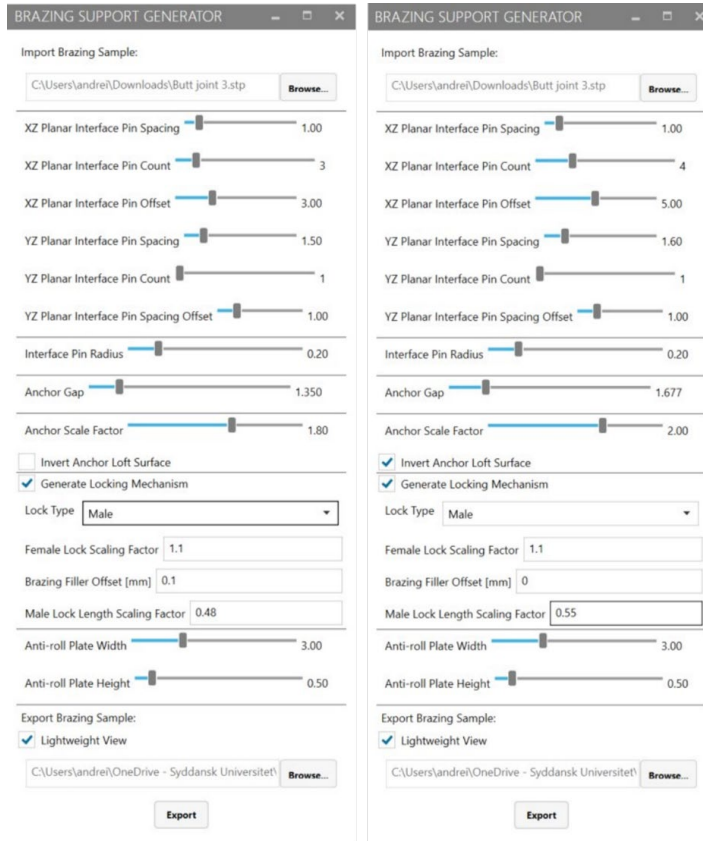


Figure 3 - V1 (left) and V2 (right) example set, with differences on offset, lock scale factor, pin count and spacing

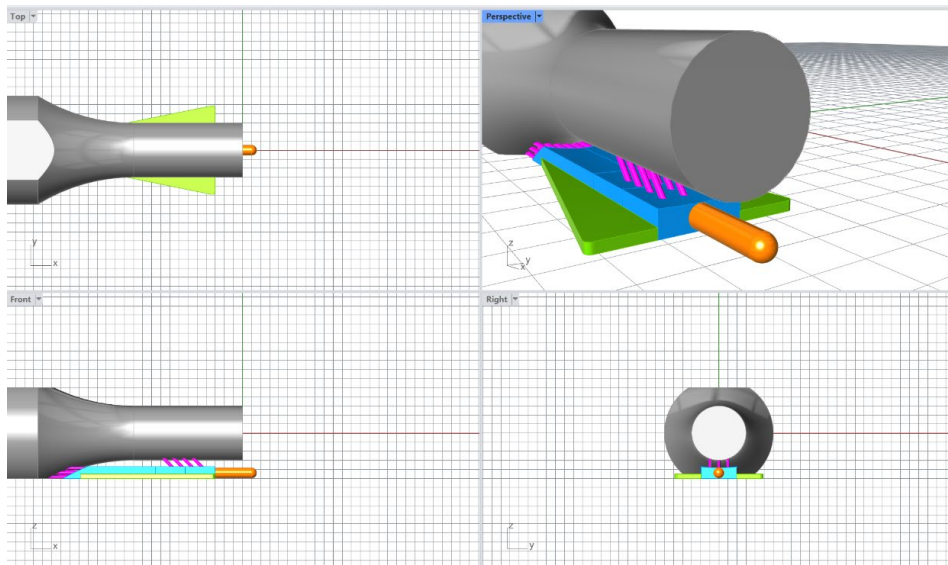


Figure 4 – Rhino views of V2 male specimen, including elongated interface pins and an upscaled locking mechanism

Targeting both torch and vacuum brazing with their inherently different filler gap requirements, the workflow incorporates a feature to adjust the offset between the butt-lap faces. Figure 5 illustrates an example of a different assembly gap of 0.11 mm measured in a Siemens NX CAD environment, after export.

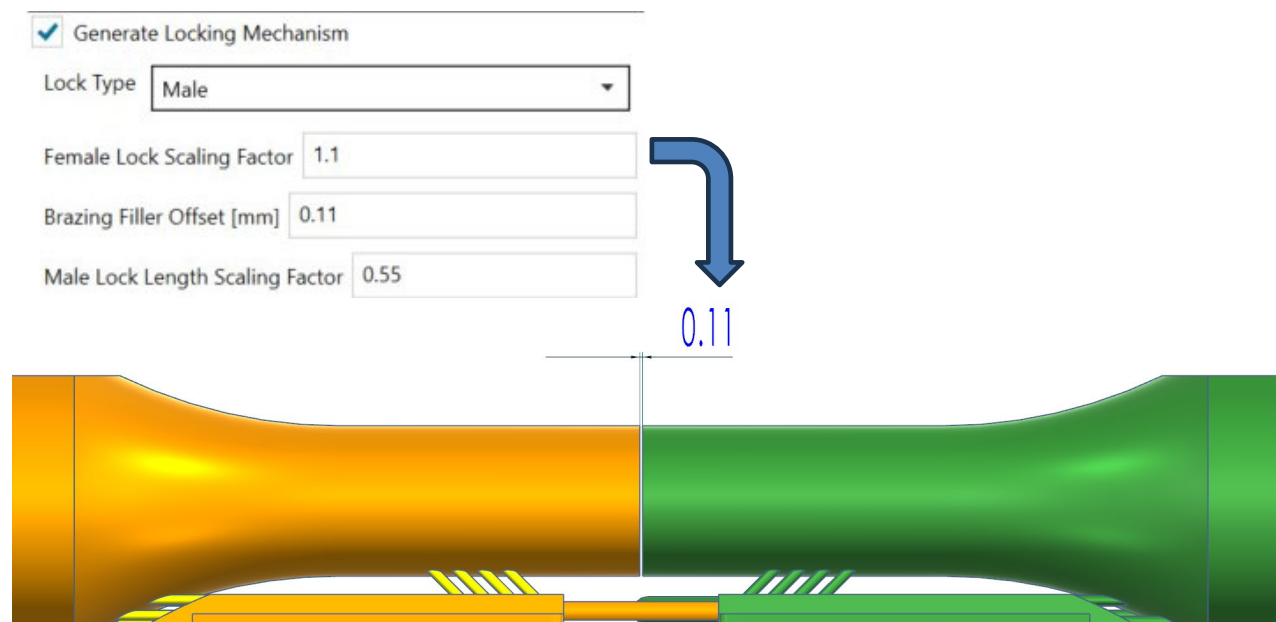


Figure 5 - CAD measurement of exported assembly

Furthermore, locking mechanisms were scaled accordingly to match the offset specifications. The final STL files for all configurations were generated successfully for a dogbone specimen of length X mm and gauge width Y mm. After L-PBF manufacturing at 195 W, scanning speed of 1000mm/s, a 30 μm layer height and a hatch distance of 0.08 mm.

In spite of the offset allowing for vacuum brazing film insertion, all samples were torch brazed using a standard film filler material. During the process, parameter group V1, which had shorter interface pins and a looser tolerance in the locking mechanism, resulted in comparatively poorer alignment and demonstrated unwanted filler material migration into the pin interface region. In contrast, V2, which featured longer, more stabilizing pins and tighter locking tolerances, preserved joint alignment more effectively and minimized filler overflow (as per Figure 6). With respect to the artefacts left on the surface after removal, their impact was not qualified, but is expected to be negligible. It is, however, important to consider the contact region between the sample and the interface pins, and that choice is made relative to the standard set of support generated by the Magics software – for 316L SS, orbiting between 0.2 and 0.7mm in diameter. A natural next step is alternating the pin geometry to more loyally replicate that of fractured supports in slicing software, with the incentive of finding the best compromise between contact area (with subsequent removal in mind) and the thermally conductive role of these structures during L-PBF manufacturing.

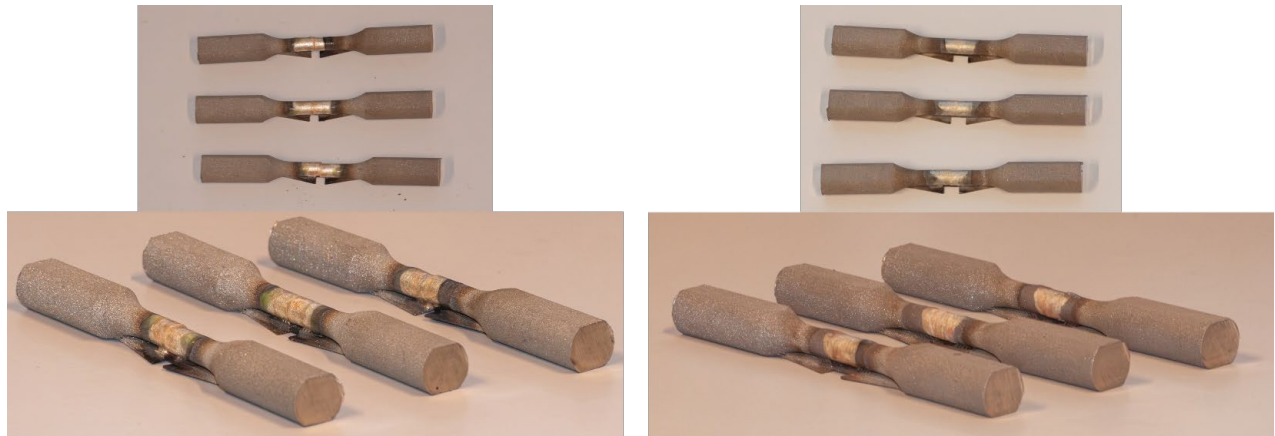


Figure 6 - V1 (left) and V2 (right) samples post brazing, with visual differences in inferior alignment and filler flow for V1

Following brazing, the support structures were mechanically removed without power tools, only using a pair of pliers, as intended. The V1 samples, for which the filler flowed down to the interface pins, bonding them to the dogbone structure, were slightly more difficult to process, and left mild artefacts on the surface. The cleaned samples were then subjected to tensile testing on a Lloyd LD30 machine equipped with a 30 kN load cell. Tests followed a 5.6 N preload at 21 mm/min, with an extension rate of 2.5 mm/min, in accordance with standard test procedures. The samples were pulled to failure to assess joint integrity, as depicted in Figure 7.

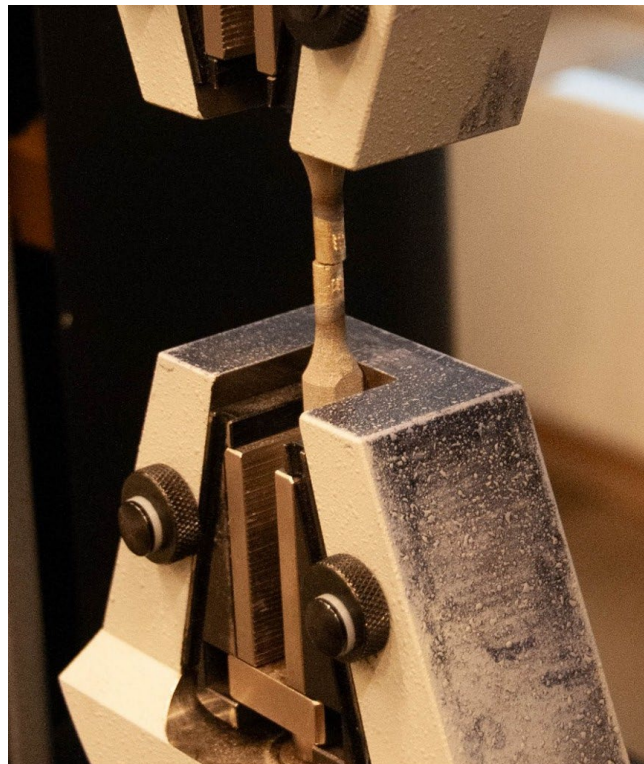


Figure 7 - Tensile fracture of V1 specimen including artefacts on the surface due to suboptimal filler flow

As shown in Figure 8, all samples demonstrated cohesive fracture behavior within the brazed joint region. While absolute tensile strength values varied, V2 samples slightly outperformed V1, with higher strength and more uniform fracture surfaces, indicating more homogeneous brazed joints. The differences, while preliminary, suggest that parameter tuning within the workflow impacts not only geometrical alignment but also mechanical quality of the resulting joints.

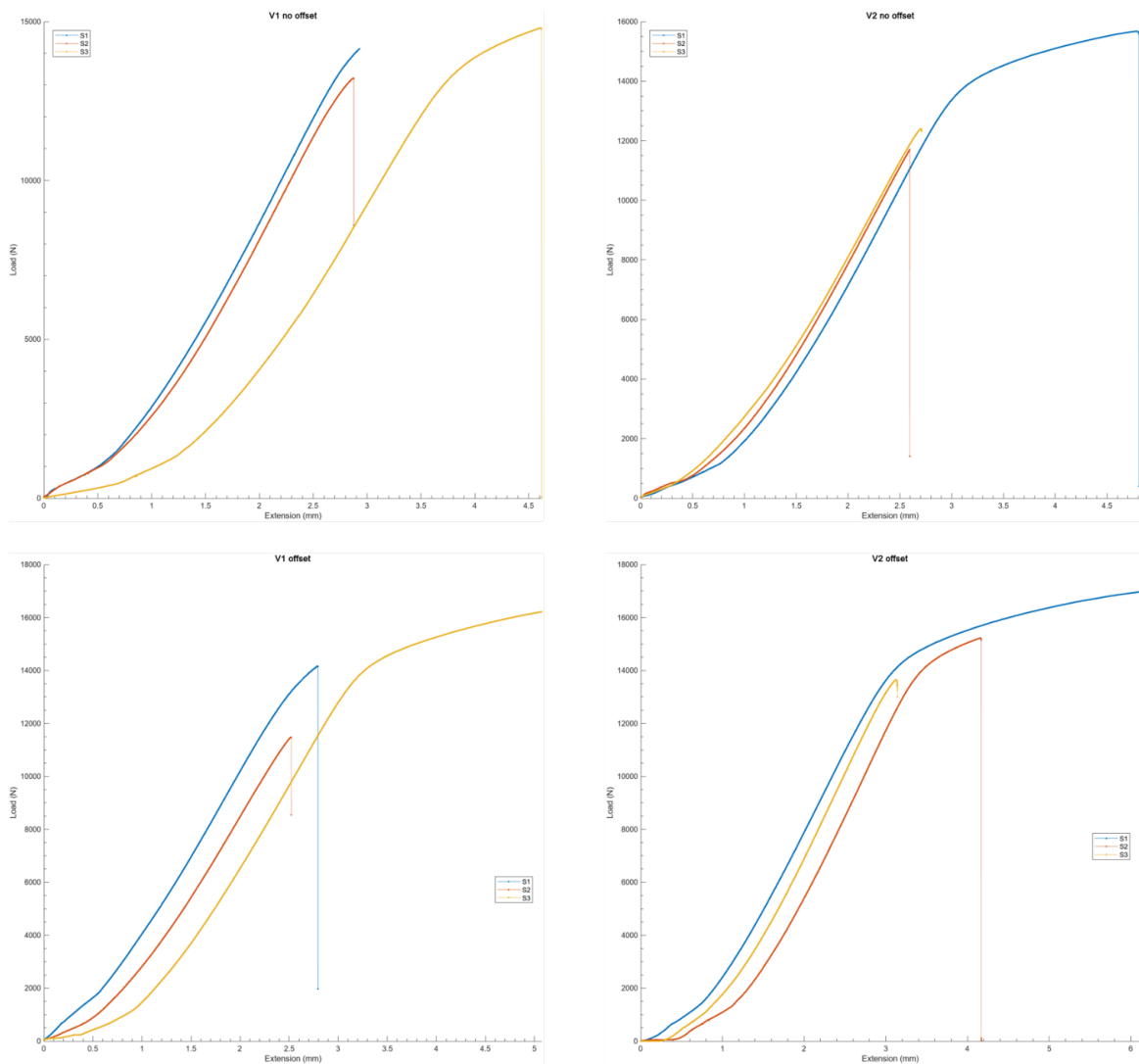


Figure 8 - Tensile results for V1 and V2 with no offset (top left and right), and V1 and V2 with 0.1 mm offset (bottom left and right)

The relative inconsistency of the stress-strain response can be attributed to the torch brazing quality itself, a manual process with no feedback other than the limited experience of the technician. The small cross-section of the interface further complicates the repeatability. Nevertheless, this trial confirms that the proposed method generates mechanically testable, structurally coherent brazed components suitable for experimental workflows.

Conclusion

This study demonstrates a semi-automated workflow for the design and fabrication of self-supporting metal 3D printed assemblies for torch and vacuum brazing, with a focus on tensile specimen butt joints as a scalable test case. By leveraging visual programming in Grasshopper and integrating four customizable support features, we successfully generated STL files with embedded alignment and sacrificial structures in minutes, significantly accelerating the design-to-fabrication process.

The ability to create application-specific support geometries—including anchor bases, breakaway pins, anti-roll fins, and locking joints—enables precise control over part alignment and joint interface quality during brazing. Furthermore, the recoverability and re-powderization potential of sacrificial features addresses waste concerns. While parameters values have been chosen loosely, their impact on the process is testimony to their importance, even in the case of small variations.

Experimental results from tensile testing confirm that brazed specimens generated via this method are mechanically testable, and that parameter tuning measurably impacts joint strength and quality. These findings open the door for future studies exploring fully automated workflows with machine learning integration, as well as scaling to complex monolithic assemblies, such as those used in fusion systems.

Acknowledgement

We would like to acknowledge Casper Andersen Tang for his help with brazing the specimens.

References

- Chi, H., Wang, X., & Jiao, Y. (2015). BIM-Enabled Structural Design: Impacts and Future Developments in Structural Modelling, Analysis and Optimisation Processes. *Arch Computat Methods Eng* 22, 135-151.
- Dryden, I. (1982). *The efficient use of energy*. Oxford, UK: Butterworth-Heinemann.
- Ebnesajjad, S. (2014). *Surface treatment of materials for adhesive bonding*. Norwich, NY, USA: William Andrew.
- F. Delzendehrooy, A. A.-S. (2022). A comprehensive review on structural joining techniques in the marine industry. *Composite structures*.
- Fang, J., Xie, M., Zhang, J., Hu, J., Liu, G., Zhao, S., . . . Jin, Q. (2024). Optimized design of composition and brazing process for Cu-Ag-Zn-Mn-Ni-Si-B-P alloy brazing material based on machine learning strategy to improve brazing properties. *Materials Today Communications* 39, 109317.
- Grasshopper3D. (2025, June). *Grasshopper 3D*. Retrieved from <https://www.grasshopper3d.com/>
- Lanzutti, A., & Marin, E. (2024). The Challenges and Advances in Recycling/Re-Using Powder for Metal 3D Printing: A Comprehensive Review. *Metals*.
- Liao, W., Lu, X., Fei, Y., Gu, Y., & Huang, Y. (2024). Generative AI design for building structures. *Automation in Construction* 157, 105187.
- Martin, D. (1968). *Method of brazing aluminum to stainless steel for high-stress-fatigue applications*. Washington D.C.: NASA Office of Technology Utilization.
- NASA. (2025, July 10). *Goddard Engineering and Technology Directorate*. Retrieved from Generative Design: <https://etd.gsfc.nasa.gov/capabilities/capabilities-listing/generative-design/>
- Roberts, P. (2013). *Industrial Brazing Practice, 2nd Ed*. Boca Raton: CRPress.
- Sandvik. (2025, 06). *Sandvik Osprey® 316L Datasheet*. Retrieved from <https://www.metalpowder.sandvik/en/products/metal-powder-alloys/austenitic-stainless-steel/osprey-316l/>
- Xact Metal. (2025, June). *Xact Metal XM200G*. Retrieved from Xact Metal Products: <https://xactmetal.com/xm200g-affordable-metal-3d-printing/>